Sensitive Detection of MicroRNA in Complex Biological Samples via Enzymatic Signal Amplification Using DNA Polymerase Coupled with Nicking Endonuclease

ARTICLE *in* ANALYTICAL CHEMISTRY · NOVEMBER 2013

Impact Factor: 5.64 · DOI: 10.1021/ac403302a · Source: PubMed

3 AUTHORS, INCLUDING:

Bin-Cheng Yin
East China University of Science & Technology
48 PUBLICATIONS **1,272** CITATIONS
SEE PROFILE

Bang-Ce Ye
East China University of Science and Technology
134 PUBLICATIONS **2,344** CITATIONS
SEE PROFILE

analytical chemistry

Article

pubs.acs.org/ac

Sensitive Detection of MicroRNA in Complex Biological Samples via Enzymatic Signal Amplification Using DNA Polymerase Coupled with Nicking Endonuclease

Bin-Cheng Yin, Yu-Qiang Liu, and Bang-Ce Ye*

Lab of Biosystem and Microanalysis, State Key Laboratory of Bioreactor Engineering, East China University of Science & Technology, Shanghai 200237, P. R. China

Supporting Information

ABSTRACT: MicroRNA (miRNA) has become an ideal biomarker candidate for cancer diagnosis, prognosis, and therapy. In this study, we have developed a novel one-step method for sensitive and specific miRNA detection via enzymatic signal amplification and demonstrated its practical application in biological samples. The proposed signal amplification strategy is an integrated "biological circuit" designed to initiate a cascade of enzymatic polymerization reactions in order to detect, amplify, and measure a specific miRNA sequence by using the isothermal strand-displacement property of a mesophilic DNA polymerase together with the nicking activity of a restriction endonuclease. The circuit is composed of two molecular switches operating in series: the nicking endonuclease-assisted isothermal polymerization reaction activated by a specific miRNA and the strand-displacement polymerization reaction designed to initiate molecular beacon-assisted amplification and signal transduction. The hsa-miR-141 (miR-141) was chosen as a target miRNA because its level specifically elevates in prostate cancer. The proposed method allowed quantitative sequence-specific detection of miR-141 in a dynamic range from 1 fM to 100 nM, with an excellent ability to discriminate differences among miR-200 family members. Moreover, the detection assay was applied to quantify miR-141 in cancerous cell lysates. The results are in excellent agreement with those from the reverse transcription polymerase chain reaction method. On the basis of these findings, we believe that this proposed sensitive and specific assay has great potential as a miRNA quantification method for use in biomedical research and clinical diagnosis.

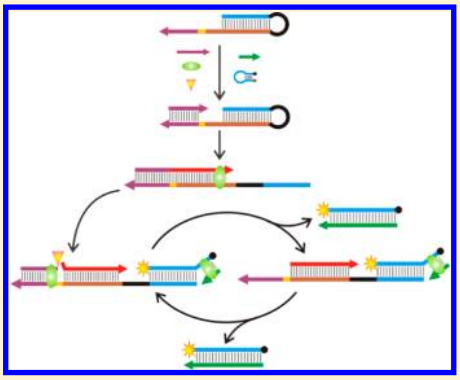

MicroRNA (miRNA) is a short endogenous, noncoding ribonucleic acid molecule (≈ 22 nucleotides) that is frequently dysregulated in various types of human cancers.[1,2] Growing evidence has demonstrated that miRNA is a promising class of tissue-based biomarker for cancer classification, diagnosis, and prognosis.[3−5] However, the intrinsic characteristics of miRNA, including its short size, sequence homology among family members, low abundance in total RNA samples, and susceptibility to degradation, complicate the accurate quantification of miRNA. Many bioanalytical methods have been developed to identify and quantify miRNA, such as Northern blotting,[6] microarrays,[7,8] and real-time polymerase chain reaction (PCR).[9−12] Among these methods, Northern blotting was regarded as the standard method for miRNA analysis in early miRNA profiling studies; however, it is not satisfactory because it has low sensitivity, is time-consuming, and complicated and large amounts of the sample are required. Microarray technology requires expensive instruments and has low sensitivity and poor specificity. The problems in the currently used PCR methods are related to precise control of temperature cycling and difficulty in the design of PCR primers. Therefore, the development of new methods that can complement and improve current approaches for sensitive, selective, and quantitative detection of miRNA at a constant temperature is urgently required.

Recently, various isothermal enzyme-assisted amplification strategies have been developed and applied to miRNA analysis. Isothermal enzyme-assisted amplification of recognition events is a powerful component for the improvement of the sensitivity of bioanalysis at a constant temperature. Usually, isothermal enzyme-based amplification methods are divided into two broad categories: linear amplification and nonlinear amplification. In contrast to the traditional hybridization assay at a target-to-signal ratio with 1:1 stoichiometry, nuclease-catalyzed target recycling strategies utilize a "catalyst" to interact with multiple probes and achieve linear signal amplification. For example, duplex-specific nuclease[13] and DNase I[14] have been employed as cleavage enzymes in miRNA recycling-oriented amplification. Despite their simple design and efficient enzymatic reaction, nuclease-assisted linear amplification methods are not as sensitive as nonlinear amplification methods. In particular, considering that trace amounts of miRNA are present in serum and precious tissue samples,

Received: August 23, 2013
Accepted: November 6, 2013
Published: November 6, 2013

dx.doi.org/10.1021/ac403302a | *Anal. Chem.* 2013, 85, 11487−11493

Table 1. Sequence Information for the DNA Oligonucleotides, MB Probe, and miRNAs Used in This Study

name	sequences* (5′-3′)
template1 for miR-141	GTGTAATGGGCGCACCTCTCTTTACTGTGTC-SPACER18-CACACAGTAAAGAGA GGTGCGCCCATTACACTGTTCATCAGGAGACCCATCTTTACCAGACAGTGTTA
template2 for let-7a	GTGTAATGGGCGCACCTCTCTTTACTGTGTC-SPACER18-CACACAGTAAAGAGA GGTGCGCCCATTACACTGTTCATCAGGAGACAACTATACAACCTACTACCTCA
primer	TCTTGGAC
MB probe	FAM-TCTTGGACACAGTAAAGAGAGGTGCGCCCATTGTGTCCAAGA-DABCYL
cMB probe	TCTTGGACACAATGGGCGCACCTCTCTTTACTGTGTCCAAGA
miR-141	UAACACUGUCUGGUAAAGAUGG
miR-429	UAAUACUGUCUGGUAAAACCGU
miR-200a	UAACACUGUCUGGUAACGAUGU
miR-200b	UAAUACUGCCUGGUAAUGAUGA
miR-200c	UAAUACUGCCGGGUAAUGAUGGA
let-7a	UGAGGUAGUAGGUUGUAUAGUU
let-7b	UGAGGUAGUAGGUUGUGUGGUU
let-7d	AGAGGUAGUAGGUUGCAUAGUU
let-7e	UGAGGUAGGAGGUUGUAUAGU

nonlinear amplification methods with high efficiency are preferable. Among the nonlinear amplification strategies, isothermal exponential amplification reaction (EXPAR) using DNA polymerase and nicking endonuclease, first devised by Galas and co-workers,[15] has found wide application in miRNA detection. On the basis of this strategy, our group recently developed a series of methods for quantitative detection of miRNA using catalytic G-quadruplex DNAzyme[16] or fluorescent metal nanoclusters for signal output.[17−19] These methods demonstrated high sensitivity because of the high amplification efficiency of EXPAR, but they all need two steps (i.e., exponential amplification reaction and signal production), which involve cumbersome handling procedures and vulnerability to contamination.

In the present study, we have described our ongoing effort to develop a novel, simple, and one-step method for sensitive detection of miRNA via an enzymatic signal amplification strategy using DNA polymerase and nicking endonuclease together. The proposed method is based on the inherent signal-transduction mechanism of fluorescence molecular beacon (MB) probes under the joint actions of the isothermal strand-displacement property of polymerase and nicking activity of restriction endonucleases. This beacon-assisted detection amplification strategy is an integrated "biological circuit" designed to detect, amplify, and measure a specific miRNA sequence in one step. The biological circuit integrates two reactions operating in series. The first reaction is a nicking endonuclease-assisted isothermal polymerization reaction activated by a specific miRNA. The second reaction is a strand-displacement polymerization reaction designed to initiate MB-assisted amplification and signal transduction. By combining polymerase strand extension, single-strand nicking, strand displacement, and MB open, this method can quantitatively detect sequence-specific miRNA in a dynamic range from 1 fM to 100 nM with a detection limit as low as 1 fM. Moreover, this method also demonstrates high selectivity for discriminating differences between miRNA family members and good performance in practical application in a complex biological matrix. Notably, the isothermal condition significantly reduces the analytical cost and simplifies the handling procedures.

EXPERIMENTAL SECTION

Reagents and Materials. The oligonucleotide probes and MB probe were custom-synthesized by Sangon, Inc. (Shanghai, China). HPLC-purified miRNAs were custom-synthesized by Takara Biotechnology Co. Ltd. (Dalian, China). The sequences of DNA oligonucleotides, the MB, and miRNAs are listed in Table 1. The nicking endonuclease *Nt.BsmAI* was purchased from New England Biolabs, Inc. (Beverly, MA). The RNase inhibitor and the polymerase Klenow fragment, exo$^-$, were purchased from Thermo Fisher Scientific, Inc. (Waltham, MA). To create and maintain an RNase-free environment, the solutions were treated with 0.1% diethyl pyrocarbonate (DEPC) and autoclaved. The tips and tubes were RNase-free and did not require pretreatment to inactivate RNases. The buffers for cell experiments were prepared using distilled water purified by a Milli-Q water purification system (Millipore Corp., Bedford, MA) with an electrical resistance of 18.2 MΩ·cm. The buffers used in cellular extracts were prepared as follows: Buffer A contained 10 mM 4-(2-hydroxyethyl)-1-piperazineethanesulfonic acid (HEPES) (pH 7.9), 1.5 mM $Mg(NO_3)_2$, 10 mM KNO_3, and 0.5 mM dithiothreitol (DTT). Buffer B contained 20 mM HEPES (pH 7.9), 25% (v/v) glycerol, 0.42 M $NaNO_3$, 1.5 mM $Mg(NO_3)_2$, 0.2 mM ethylenediaminetetraacetic acid (EDTA), 0.5 mM phenylmethylsulfonyl fluoride (PMSF), and 0.5 mM DTT. Buffer C contained 20 mM HEPES (pH 7.9), 20% (v/v) glycerol, 0.1 M KNO_3, 0.2 mM EDTA, 0.5 mM PMSF, and 0.5 mM DTT.

Instrumentation. Fluorescence emission spectra were recorded by using a fluorescence microplate reader (Bio-Tek Instruments, Winooski, VT) and a black 384-well microplate (Fluotrac 200, Greiner, Germany). The results of polyacrylamide gel electrophoresis were visualized with an FR-200A instrument (Shanghai, China). Quantitative real-time PCR analysis was conducted using the Bio-Rad CFX96 Real-Time PCR Detection System (Hercules, CA) and TaKaRa kits (One Step PrimeScript miRNA cDNA Synthesis Kit and SYBR Premix Ex *Taq*II kit) (TaKaRa, Dalian, China). The threshold cycle (C_t) in quantitative real-time PCR was calculated using CFX software version 1.1 (Bio-Rad, Hercules, CA).

Preparation of Cellular Extracts. A human pancreatic cancer cell line (AsPc-1), human prostate carcinoma cell lines (22Rv1 and DU 145), a human hepatocellular carcinoma cell line (BEL-7404), a human cervical cancer cell line (HeLa), and a human breast cancer cell line (MDA-MB231) were obtained from the cell bank of the type culture collection of the Chinese Academy of Sciences (Shanghai, China). AsPc-1 cells, 22Rv1 cells, and DU 145 cells were cultured at 37 °C in a humidified

5% CO_2 incubator in RPMI medium 1640 supplemented with 10% fetal bovine serum (FBS) and 100 U/mL penicillin−streptomycin. HeLa cells, MDA-MB231 cells, and BEL-7404 cells were cultured at 37 °C in a humidified 5% CO_2 incubator in Dulbecco's Modified Eagle Medium (DMEM) supplemented with 10% fetal bovine serum (FBS) and 100 U/mL penicillin−streptomycin. The cells were grown in fresh medium in 50 mm glass-bottom dishes. The cells were then harvested by trypsinization, washed with fresh medium three times, and finally suspended in fresh medium for the following experiments. The cellular extracts were prepared according to a previously reported method with minor modifications.[20] Briefly, the collected cells were washed once with phosphate-buffered saline and twice with Buffer A. The cell pellet was suspended in Buffer B/0.1% Nonidet P-40 (20 μL per 10^7 cells). After incubation for 15 min on ice, the cellular suspension was briefly mixed on a vortex and centrifuged for 10 min at 4 °C. Then, the supernatant was diluted with 80 μL of Buffer C per 10^7 cells and stored at −80 °C.

miRNA Detection Procedures. The reaction mixtures for the isothermal polymerization reaction were prepared separately as a part A solution and part B solution. The part A solution consisted of 100 nM template, 250 μM deoxynucleotide triphosphates (dNTPs), 50 nM primer, 10× annealing buffer (100 mM Tris-HCl, pH 8.0 at 25 °C, 500 mM KAc, and 10 mM EDTA), miRNA, and DEPC-treated H_2O in a volume of 17 μL. The part B solution consisted of 0.32 U/μL RNase inhibitor, 0.2 U/μL nicking endonuclease *Nt.BsmAI*, 0.3 U/μL polymerase Klenow fragment, exo$^-$, 5× reaction buffer (250 mM Tris-HNO_3, 6 mM $MgCl_2$, 5 mM DTT, 50 mM KAc, pH 8.8 at 25 °C, and 30% dimethyl sulfoxide), and 80 nM MB probe in a volume of 8 μL. First, the part A solution was incubated at 88 °C for 10 min; then, the temperature was reduced from 88 to 38 °C in a decrement of 2 °C. Then, the part A solution was incubated at 37 °C for 10 min. Subsequently, part A and part B were mixed, and the polymerization reaction was performed in a volume of 25 μL at 37 °C for 60 min. After the reaction, the resultant mixture was mixed with 55 μL of H_2O and scanned using a fluorescence microplate reader from 500 to 650 nm under excitation at 480 nm. Unless noted otherwise, all experiments for miRNA measurements were repeated three times in this study.

RESULTS AND DISCUSSION

The working principle of the proposed method for specific miRNA detection based on the cascade enzymatic amplification strategy is illustrated in Scheme 1. The reaction system consists of a hairpin template, a short primer, an MB, mesophilic DNA polymerase, and nicking endonuclease. The hairpin template includes an overhang nucleic acid segment (denoted in violet in Scheme 1) complementary to the target miRNA, a specific sequence (5′-CAGAGG-3′, denoted in yellow in Scheme 1) for the recognition site of the nicking endonuclease *Nt.BsmAI*, and a stem structure formed by two complementary sequences linked by a 18-carbon spacer (denoted in black in Scheme 1). Although one arm (denoted in blue in Scheme 1) of the stem structure is complementary to the 5′ part of the MB, it is designed to be blocked by hybridization with another arm of the stem (denoted in brown in Scheme 1). This method involves two molecular switches that operate in series at a constant temperature. The first switch is the nicking endonuclease-assisted isothermal polymerization reaction activated by a specific miRNA. The second switch is the strand-displacement polymerization reaction designed to initiate MB-assisted amplification and signal transduction. Upon the interaction of the overhang region of the hairpin template with the miRNA target, the first polymerization reaction is initiated in the presence of DNA polymerase and dNTPs. Then, a double-stranded DNA with a recognition site for the nicking endonuclease is produced that would stop at the site of the 18-carbon spacer block, resulting in a conformational change of the hairpin template. The stem of the hairpin template is opened. Subsequently, the second polymerization reaction is activated. The separated arm (denoted in blue in Scheme 1) of the hairpin template binds to a complementary sequence of the MB, causing its conformation switch and fluorescence restoration. As a result of the activation, the primer anneals with the open stem of the MB and triggers a new polymerization reaction. As the primer extends, the separated arm of the hairpin template is displaced under the strand-displacement activity of the polymerase. Then, a complementary DNA is synthesized to form a beacon-cDNA complex, whereas the separated arm of the hairpin template is free to hybridize with a new MB and initiate a new cycle of triggering, priming, and displacement, which would produce a great amount of beacon−cDNA complexes. At the same time, the first switch is continuously generating a large amount of the DNA trigger (denoted in red in Scheme 1) to open hairpin templates in a single reaction cycle; as a result, the nicking endonuclease nicks the upper replicated strand to release a short fragment from the amplification template generated by the polymerase with its strand-displacement activity. Correspondingly, the second switch is initiated by the DNA triggers generated from the first switch. Therefore, the proposed cascade enzymatic amplification method presents a significant increase in fluorescence signal that is proportional to the concentration of target miRNA.

Scheme 1. Schematic Illustration of Enzyme-Assisted Amplified Detection Of Specific miRNA Based on DNA Polymerase and Nicking Endonuclease

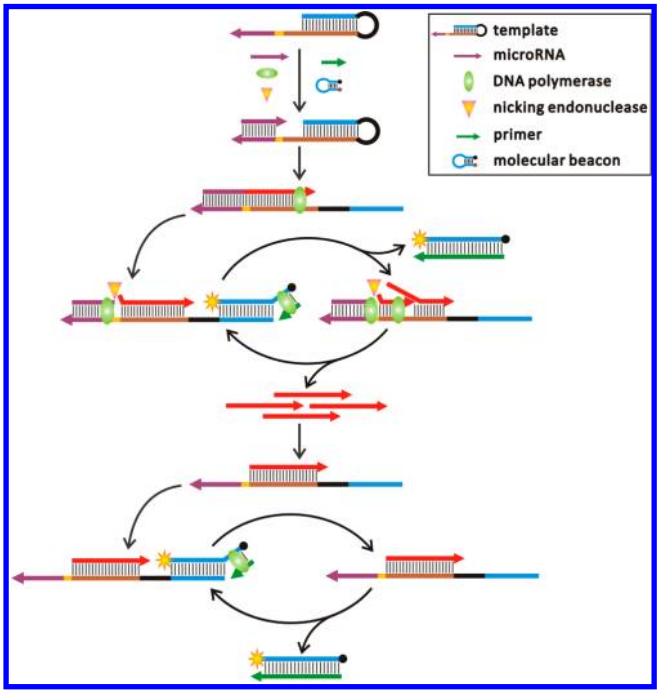

dx.doi.org/10.1021/ac403302a | *Anal. Chem.* 2013, 85, 11487−11493

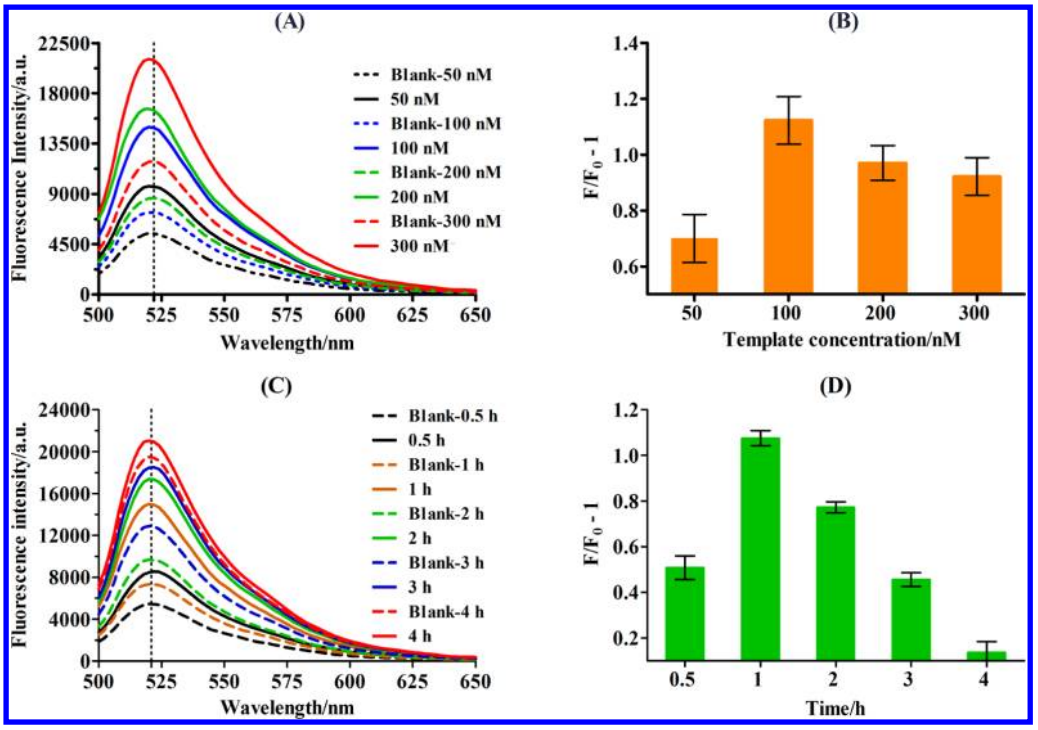

Figure 1. Effects of template concentration and reaction times on the performance of the proposed method. (A) Fluorescence emission spectra responses to templates with different concentrations in the absence and the presence of miR-141. (B) Bar representing fluorescence ratio (F/F_0-1) responses in the presence of the template with different concentrations. (C) Fluorescence emission spectra responses to the different reaction times in the absence and presence of miR-141. (D) Bar representing fluorescence ratio (F/F_0-1) responses in the presence of different reaction times. F and F_0 are the fluorescence intensities at a peak value of 520 nm in the presence and absence of miR-141, respectively. The concentration of miR-141 tested here was 10 pM. The error bars represent the standard deviations of three parallel tests.

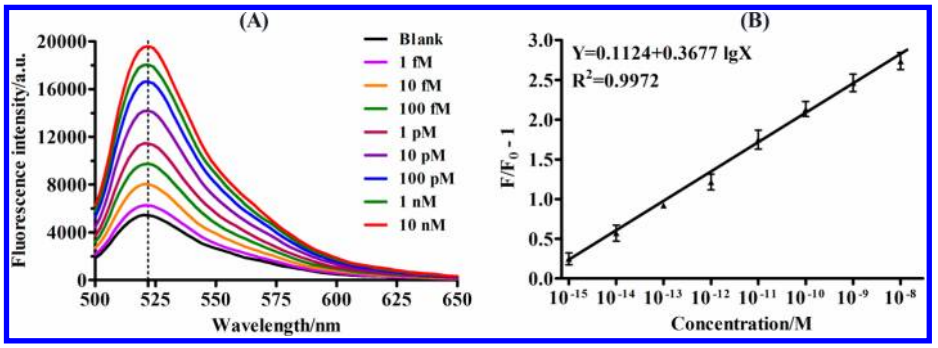

Figure 2. Sensitivity investigation of the proposed method for the target miR-141. (A) Fluorescence emission spectrum responses to excitation at 480 nm in the presence of miR-141 at different concentrations (0, 1 fM, 10 fM, 100 fM, 1 pM, 10 pM, 100 pM, 1 nM, and 10 nM) spiked in DEPC-treated water. (B) Plot of the relationship between the fluorescence ratio (F/F_0-1) at the peak value of 520 nm and the logarithm of the concentration of miR-141. The error bars represent the standard deviations of three parallel tests.

To explore the feasibility of the proposed method, we selected hsa-miR-141 (miR-141) as a model to optimize the experimental conditions. miR-141 is a member of the miR-200 family, which is an epithelial-associated miRNA family expressed in a wide range of common human cancers including breast, lung, colon, and prostate.[21] The polymerization reaction usually promises ultrahigh sensitivity, but the sensitivity and detection limits of polymerization reactions are mainly hindered by nonspecific background amplification, which especially appears to be affected by the concentration of the template and amplification time. Thus, we investigated the amount of template and the reaction time required to obtain optimal detection performance. In this study, the fluorescence ratio (F/F_0-1) was employed to evaluate the performance of the test factors, where F and F_0 are the fluorescence intensities at 520 nm under excitation at 480 nm obtained from the presence and the absence of miR-141, respectively. It should be noted that a higher fluorescence ratio (F/F_0-1) value is more favorable to obtain higher sensitivity of the detection method. We first investigated the template concentration for four concentrations of 50, 100, 200, and 300 nM. As shown in Figure 1A, the fluorescence emission spectra with different template concentrations in the absence and the presence of miR-141 were recorded. It is clear that the background signal was strongly dependent on the initial concentration of template. With increasing template concentrations, the background signal and the corresponding signals were also increased. This significant increase in background signal is attributable to the common phenomenon of nonspecific background amplification. The reasons may be primer/

dx.doi.org/10.1021/ac403302a | Anal. Chem. 2013, 85, 11487−11493

template-independent polymerization, false priming at sites where primer dimers are formed, nonspecific opening of the MB, or inherent technical difficulty.[22] To discriminate the signal from noise to achieve good sensitivity, we chose 100 nM template obtained using the highest fluorescence ratio (F/F_0-1) value (Figure 1B) for the subsequent experiments. The influence of amplification time was further investigated. Five reaction times of 0.5, 1, 2, 3, and 4 h were chosen. Figure 1C,D show the fluorescence emission spectra and fluorescence ratio (F/F_0-1) responses to different reaction times in the absence and the presence of miR-141. Similar to the phenomenon observed for template concentration, the background signal and corresponding signal also increased with an increase in reaction times. The highest fluorescence ratio (F/F_0-1) value was achieved at a reaction time of 1 h, which was thus chosen for further experiments. In addition, we also investigated the effect of MB concentration on the performance of the proposed method and selected 80 nM MB for the following experiments (as shown in Figure S2).

Under the above optimal experimental conditions and according to the experimental protocol described in the Experimental Section, we investigated the sensitivity of the proposed method by detecting synthetic miR-141 at different concentrations (0, 1 fM, 10 fM, 100 fM, 1 pM, 10 pM, 100 pM, 1 nM, and 10 nM) prepared in DEPC-treated water. As shown in Figure 2A, fluorescence spectra were recorded upon introduction of different concentrations of target miR-141. As expected, a gradual increase in the fluorescent peak at 520 nm was clearly observed with an increase in the concentration of miR-141 from 1 fM to 10 nM. Figure 2B illustrates that the fluorescence intensity ratio (F/F_0-1) exhibited a good linear relationship with the logarithmic (lg) value of miR-141 concentration in the dynamic range from 1 fM to 10 nM. The correlation equation is $Y = 0.1124 + 0.3677\ \lg X$, with a correlation coefficient R^2 of 0.9972, where Y is the fluorescence ratio (F/F_0-1) at 520 nm and X is the concentration of miR-141. The experimentally measured detection limit for miR-141 was as low as 1 fM. To the best of our knowledge, the proposed method is superior in sensitivity to commercial kits from TaKaRa products and other homogeneous detection methods such as graphene oxide-based miRNA,[14,23] silver nanocluster DNA probes,[24] affinity-based assays,[25] and E-DNA sensors.[26] The high sensitivity achieved in the proposed method is attributed not only to the high magnitude of amplification efficiency from the joint action of DNA polymerase and nicking endonuclease but also to the successful MB-assisted strand-displacement polymerization.

Distinguishing among members from the same miRNA family is of great importance for better understanding the biological functions of individual miRNAs. Because miRNA families often possess closely related sequences with high homology, it is a great challenge to discriminate the differences between miRNA family members that differ by only a few nucleotides. To evaluate the specificity of the proposed miRNA assay, five members (miR-141, miR-429, miR-200a, miR-200b, and miR-200c) of the miR-200 family were selected for analysis with the miR-141-specific template. The resultant products of the polymerization reaction in the presence of different miRNA targets were verified by nondenaturing polyacrylamide gel electrophoresis (PAGE). To facilitate the comparison, a positive control sample of double-stranded DNA composed of the MB and its complementary strand was prepared. As shown in Figure S1, a characteristic band of reporter beacon–cDNA complexes (~42 bp) was clearly observed in the presence of miR-141, as observed in the positive control sample. In contrast, the negative control without miR-141 or the competing stimulus including miR-429, miR-200a, miR-200b, and miR-200c showed negligible bands representative of the length of 42 bp. Figure 3 presents the comparison of the

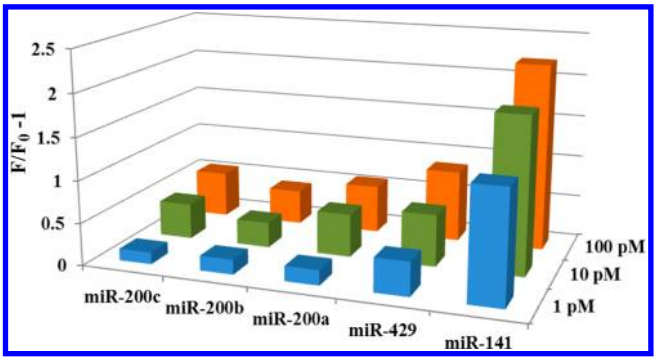

Figure 3. Selectivity investigation of the proposed method using the miR-200 family as a model system. Bars represent the fluorescence ratio (F/F_0-1) for the different targets of miR-141, miR-429, miR-200a, miR-200b, and miR-200c at three concentrations of 100, 10, and 1 pM, respectively.

fluorescence ratio (F/F_0-1) for different miRNA targets under the three concentrations of 100 pM, 10 pM, and 1 pM. As expected, the fluorescence ratio values generated by miR-141 were the highest among those produced by miR-200 members at the tested concentrations. Furthermore, we also studied the specificity of the proposed method by using let-7 miRNA family members as targets (data as shown in Figure S3). These results and the PAGE analysis clearly demonstrate that the detection method has high sequence specificity to distinguish among miRNA family members, which further supports the feasibility of the proposed method.

To investigate whether the proposed method can be applied to quantitative detection of target miRNAs in a complex biological matrix, we employed the cell lysates as model matrix. The cell lysates from six human cancer cell lines, including a hepatocellular carcinoma cell line (BEL-7404), a breast cancer cell line (MDA-MB231), prostate carcinoma cell lines (22Rv1 and DU 145), a pancreatic cancer cell line (AsPc-1), and a cervical cancer cell line (HeLa) were chosen. Before quantitation of the amount of miR-141 in the cell lysates, we spiked a series of standards with synthetic miR-141 at different concentrations (0, 1 fM, 10 fM, 100 fM, 1 pM, 10 pM, 100 pM, 1 nM, and 10 nM) in Buffer B/0.1% Nonidet P-40 and Buffer C to imitate the buffer conditions of the tested cell lysates. We then employed our method to establish the calibration curve. As shown in Figure S4B, the relationship between the fluorescence ratio value and the logarithm of the amount of miR-141 was different from that in DEPC-treated water (as shown in Figure 2B), probably because the reaction environment affects the enzymatic reaction and fluorescence signal. For comparison, commercial kits based on RT-PCR were also used to detect a series of miR-141 standards containing known concentrations (0, 100 fM, 1 pM, 10 pM, 100 pM, 1 nM, 10 nM, 100 nM, and 1 μM) in Buffer B/0.1% Nonidet P-40 and Buffer C to establish a calibration curve (as shown in Figure S5A and S5B). According to the linear calibration curves obtained, the amount of miR-141 in the six cell lysates was measured using our proposed method and the commercial kits

dx.doi.org/10.1021/ac403302a | Anal. Chem. 2013, 85, 11487–11493

(Figure S4D and Figure S5D). As shown in Figure 4, the amount of miR-141 measured by these two methods was converted to the number of copies of the miRNA molecule in a cell to permit comparisons. The results show that miR-141 had different expression levels in different cancer cell lines. The cell lysate from 22Rv1 prostate carcinoma cells had a higher concentration of miR-141 than that of other cells, which was in good accordance with a previous report of up-regulation of miR-141 in 22Rv1 cells.[21] In addition, we spiked different amounts of miR-141 with known concentrations in the cell lysates of MDA-MB231 cells and 22Rv1 cells to test the accuracy of the proposed method. The results are summarized in Table S1, which shows that recovery was in the range of 95.21−104.78%. These results clearly indicated that the proposed method has great promise for practical application with great accuracy and reliability for miRNA detection.

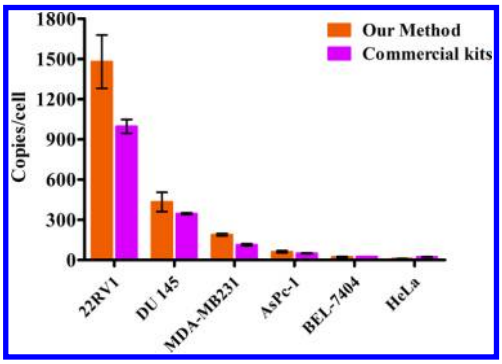

Figure 4. Practical application of miR-141 detection in cancer cell lysates of 22Rv1 cells, DU145 cells, MDA-MB231 cells, AsPc-1 cells, BEL-7404 cells, and HeLa cells. Bars represent the amount of copies of miR-141 per cell determined using our proposed method (brown bars) and commercial kits (purple bars). The error bars represent the standard deviations of three parallel tests.

CONCLUSIONS

There is still an increasing need for developing simple, highly sensitive, and selective assays for miRNA quantification, which can be used in potential applications in disease molecular diagnoses and biomedicine. In this proof-of-principle work, we have developed such a method for mature miRNA analysis in a cell lysate biological sample via enzymatic signal amplification strategy. This method relies on the cascade enzymatic polymerization reaction to initiate MB-assisted signal amplification and signal transduction by employing DNA polymerase and nicking endonuclease. Our assay has demonstrated the following remarkable advantages. Because of the high amplification efficiency attributed to the isothermal strand-displacement property of the polymerase together with the nicking activity of restriction endonuclease, the sensitivity of this method (detection limit for miR-141 is as low as 1 fM) is much higher than that of standard Northern blotting, microarray-based methods, and prevalent RT-PCR methods. The method was also found to have excellent differentiation ability for discriminating among miRNA family members, which is a very important factor in miRNA analysis. Additionally, the isothermal operation and simple fluorescence output eliminate the requirement for high-precision thermal cycling and gel analysis, which would greatly facilitate the development of a simple, low-cost, and portable detection system for point-of-care testing. Furthermore, our method has successfully achieved the detection of human miRNA from cancer cells. On the basis of the distinctive properties presented here, we believe the proposed assay holds great promise for future advances in research on the biological roles of miRNA and application of routine clinical diagnosis with miRNA as targets, particularly for early cancer diagnosis and designer drug therapy.

ASSOCIATED CONTENT

Supporting Information

Additional information as noted in the text. This material is available free of charge via the Internet at http://pubs.acs.org.

AUTHOR INFORMATION

Corresponding Author

* E-mail: bcye@ecust.edu.cn.

Notes

The authors declare no competing financial interest.

ACKNOWLEDGMENTS

This work was jointly supported by the National Natural Science Foundation of China (Grant Nos. 21335003, 21205040, and 21075040), the Shanghai Fund (12ZR1442700, 11 nm0502500), the Fundamental Research Funds for the Central Universities, and Hitachi, Ltd.

REFERENCES

(1) He, L.; Hannon, G. J. *Nat. Rev. Genet.* **2004**, *5*, 522.
(2) Manikandan, J.; Aarthi, J. J.; Kumar, S. D.; Pushparaj, P. N. *Bioinformation* **2008**, *2*, 330.
(3) Lu, J.; Getz, G.; Miska, E. A.; Alvarez-Saavedra, E.; Lamb, J.; Peck, D.; Sweet-Cordero, A.; Ebert, B. L.; Mak, R. H.; Ferrando, A. A.; Downing, J. R.; Jacks, T.; Horvitz, H. R.; Golub, T. R. *Nature* **2005**, *435*, 834.
(4) Calin, G. A.; Croce, C. M. *Nat. Rev. Cancer* **2006**, *6*, 857.
(5) Keller, A.; Leidinger, P.; Bauer, A.; Elsharawy, A.; Haas, J.; Backes, C.; Wendschlag, A.; Giese, N.; Tjaden, C.; Ott, K.; Werner, J.; Hackert, T.; Ruprecht, K.; Huwer, H.; Huebers, J.; Jacobs, G.; Rosenstiel, P.; Dommisch, H.; Schaefer, A.; Muller-Quernheim, J.; Wullich, B.; Keck, B.; Graf, N.; Reichrath, J.; Vogel, B.; Nebel, A.; Jager, S. U.; Staehler, P.; Amarantos, I.; Boisguerin, V.; Staehler, C.; Beier, M.; Scheffler, M.; Buchler, M. W.; Wischhusen, J.; Haeusler, S. F.; Dietl, J.; Hofmann, S.; Lenhof, H. P.; Schreiber, S.; Katus, H. A.; Rottbauer, W.; Meder, B.; Hoheisel, J. D.; Franke, A.; Meese, E. *Nat. Methods* **2011**, *8*, 841.
(6) Válóczi, A.; Hornyik, C.; Varga, N.; Burgyán, J.; Kauppinen, S.; Havelda, Z. *Nucleic Acids Res.* **2004**, *32*, e175.
(7) Lim, L. P.; Lau, N. C.; Garrett-Engele, P.; Grimson, A.; Schelter, J. M.; Castle, J.; Bartel, D. P.; Linsley, P. S.; Johnson, J. M. *Nature* **2005**, *433*, 769.
(8) Liu, C. G.; Calin, G. A.; Meloon, B.; Gamliel, N.; Sevignani, C.; Ferracin, M.; Dumitru, C. D.; Shimizu, M.; Zupo, S.; Dono, M.; Alder, H.; Bullrich, F.; Negrini, M.; Croce, C. M. *Proc. Natl. Acad. Sci. U.S.A.* **2004**, *101*, 9740.
(9) Chen, C.; Ridzon, D. A.; Broomer, A. J.; Zhou, Z.; Lee, D. H.; Nguyen, J. T.; Barbisin, M.; Xu, N. L.; Mahuvakar, V. R.; Andersen, M. R.; Lao, K. Q.; Livak, K. J.; Guegler, K. J. *Nucleic Acids Res.* **2005**, *33*, e179.
(10) Li, J.; Yao, B.; Huang, H.; Wang, Z.; Sun, C.; Fan, Y.; Chang, Q.; Li, S.; Wang, X.; Xi, J. *Anal. Chem.* **2009**, *81*, 5446.
(11) Raymond, C. K.; Roberts, B. S.; Garrett-Engele, P.; Lim, L. P.; Johnson, J. M. *RNA* **2005**, *11*, 1737.
(12) Yu, C. Y.; Yin, B. C.; Ye, B. C. *Chem. Commun.* **2013**, *49*, 8247.
(13) Yin, B. C.; Liu, Y. Q.; Ye, B. C. *J. Am. Chem. Soc.* **2012**, *134*, 5064.

(14) Cui, L.; Lin, X.; Lin, N.; Song, Y.; Zhu, Z.; Chen, X.; Yang, C. J. *Chem. Commun.* **2012**, *48*, 194.
(15) Van Ness, J.; Van Ness, L. K.; Galas, D. J. *Proc. Natl. Acad. Sci. U.S.A.* **2003**, *100*, 4504.
(16) Wang, X. P.; Yin, B. C.; Wang, P.; Ye, B. C. *Biosens. Bioelectron.* **2013**, *42*, 131.
(17) Liu, Y. Q.; Zhang, M.; Yin, B. C.; Ye, B. C. *Anal. Chem.* **2012**, *84*, 5165.
(18) Wang, X. P.; Yin, B. C.; Ye, B. C. *RSC Adv.* **2013**, *3*, 8633.
(19) Zhang, M.; Liu, Y. Q.; Yu, C. Y.; Yin, B. C.; Ye, B. C. *Analyst* **2013**, *138*, 4812.
(20) Osborn, L.; Kunkel, S.; Nabel, G. J. *Proc. Natl. Acad. Sci. U.S.A.* **1989**, *86*, 2336.
(21) Mitchell, P. S.; Parkin, R. K.; Kroh, E. M.; Fritz, B. R.; Wyman, S. K.; Pogosova-Agadjanyan, E. L.; Peterson, A.; Noteboom, J.; O'Briant, K. C.; Allen, A.; Lin, D. W.; Urban, N.; Drescher, C. W.; Knudsen, B. S.; Stirewalt, D. L.; Gentleman, R.; Vessella, R. L.; Nelson, P. S.; Martin, D. B.; Tewari, M. *Proc. Natl. Acad. Sci. U.S.A.* **2008**, *105*, 10513.
(22) Zou, B.; Ma, Y.; Wu, H.; Zhou, G. *Analyst* **2012**, *137*, 729.
(23) Dong, H.; Zhang, J.; Ju, H.; Lu, H.; Wang, S.; Jin, S.; Hao, K.; Du, H.; Zhang, X. *Anal. Chem.* **2012**, *84*, 4587.
(24) Yang, S. W.; Vosch, T. *Anal. Chem.* **2011**, *83*, 6935.
(25) Li, J.; Schachermeyer, S.; Wang, Y.; Yin, Y.; Zhong, W. *Anal. Chem.* **2009**, *81*, 9723.
(26) Wang, J.; Yi, X.; Tang, H.; Han, H.; Wu, M.; Zhou, F. *Anal. Chem.* **2012**, *84*, 6400.

SUPPORTING INFORMATION

Sensitive Detection of MicroRNA in Complex Biological Samples via Enzymatic Signal Amplification Using DNA Polymerase Coupled with Nicking Endonuclease

*Bin-Cheng Yin, Yu-Qiang Liu, and Bang-Ce Ye**

Lab of Biosystem and Microanalysis, State Key Laboratory of Bioreactor Engineering, East China University of Science & Technology, Shanghai, 200237, P. R. China

Corresponding author: Prof. Bang-Ce Ye, bcye@ecust.edu.cn.

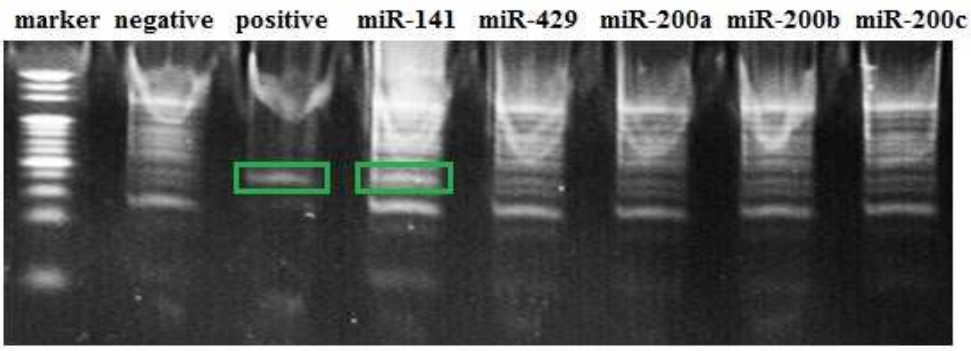

Figure S1. Non-denaturing PAGE verification of the proposed method in the presence of different miRNA targets. Lane **1**: DNA ladder marker, lane **2**: negative control (polymerization reaction without miR-141), lane **3**: positive control (double-strand DNA composed of the molecular beacon and its complementary strand), lane 4: amplification reaction with miR-141 as target, lane **5**-**8**: amplification reaction with the miR-429, miR-200a, miR-200b and miR-200c, respectively.

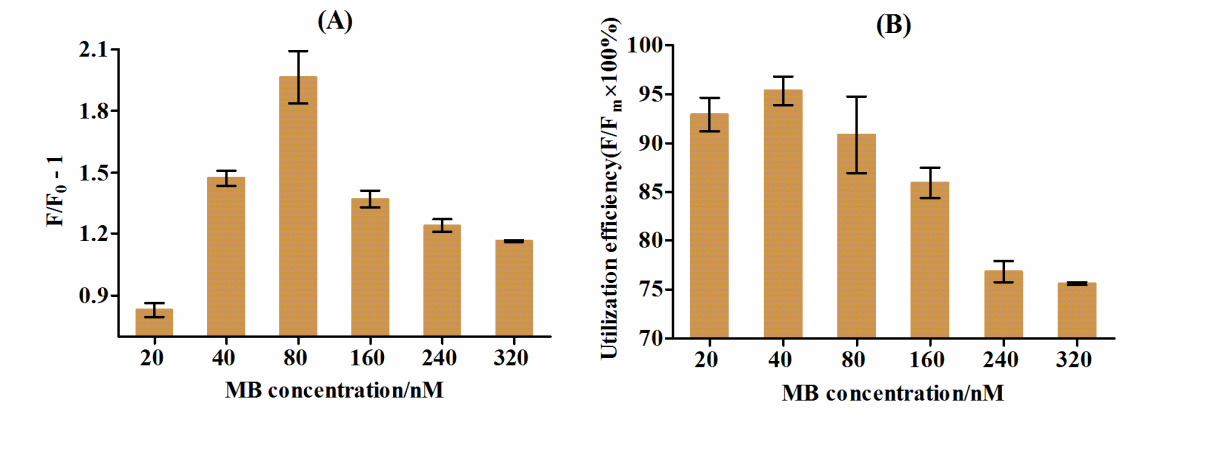

Figure S2. Selection of MB concentration. (A) Fluorescence ratio (F/F_0-1) responses to MB with different concentrations (20 nM, 40 nM, 80 nM, 160 nM, 240 nM, and 320 nM) in the presence of 10 pM miR-141. (B) Bar representing utilization efficiencies ($F/F_m\times100\%$) of MB with different concentrations. F and F_0 are the fluorescence intensities at a peak value of 520 nm in the presence and absence of 10 pM miR-141, respectively. F_m is the maximum fluorescence intensity of MB probe at the open state (at a peak value of 520 nm) in the presence of excess cMB probe (600 nM).

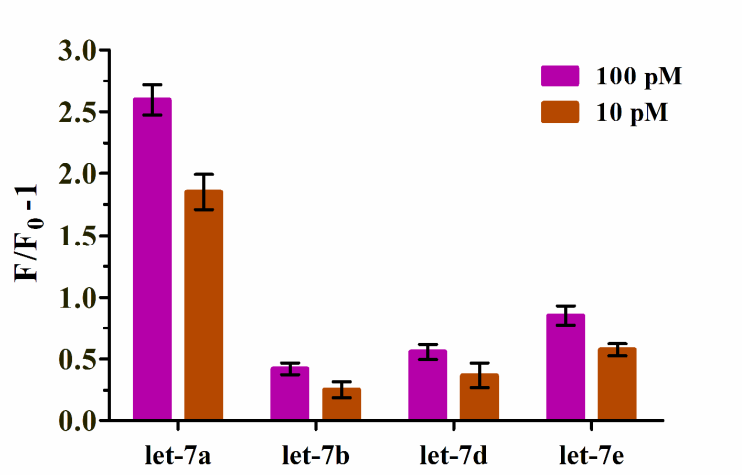

Figure S3. Selectivity investigation of the proposed method using the let-7 miRNA family as a model system. Bars represent the fluorescence ratio (F/F_0-1) for the different targets of let-7a, let-7b, let-7d, and let-7e at two concentrations of 100 pM and 10 pM.

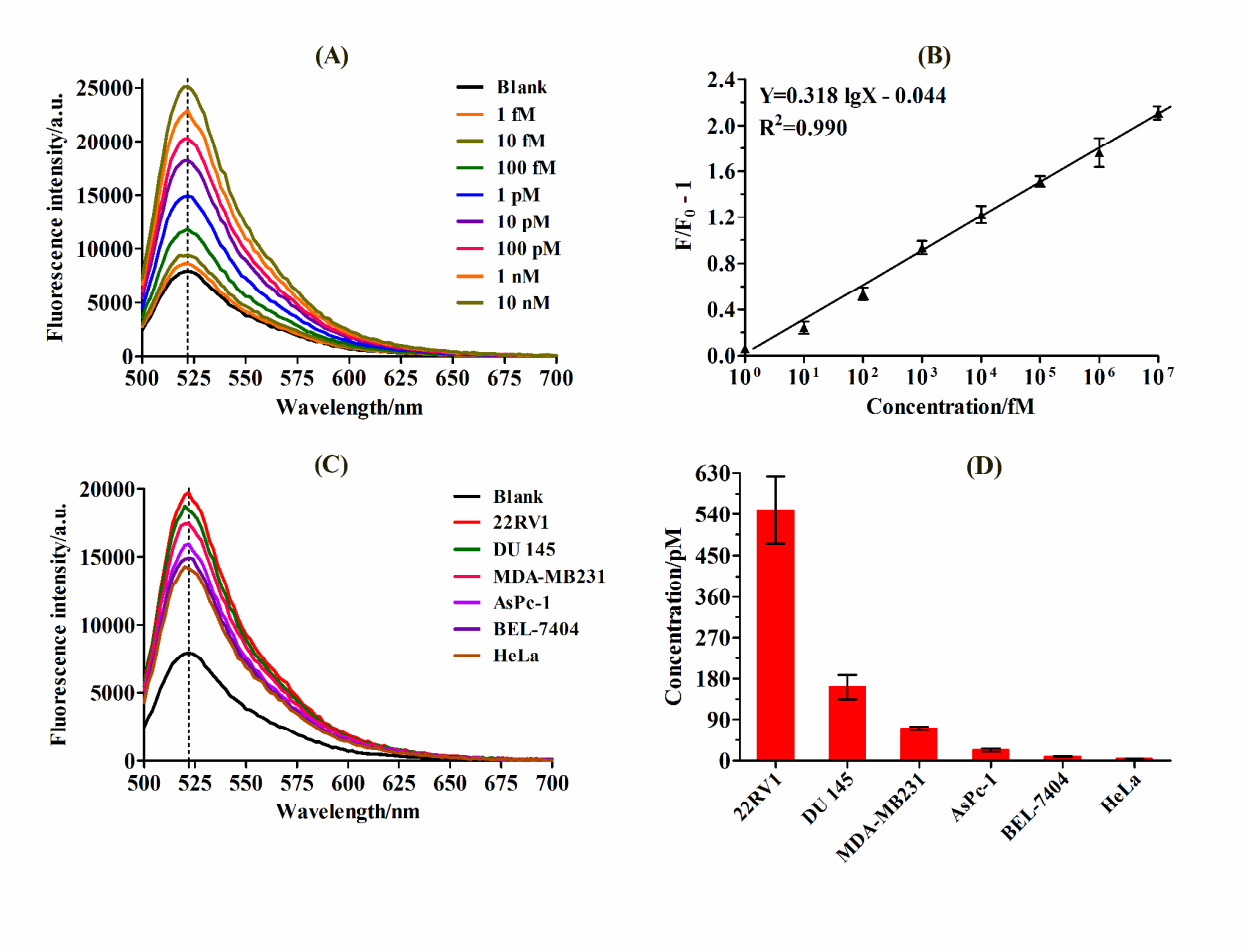

Figure S4. (A) Fluorescence emission spectra response to excitation at 480 nm in presence of miR-141 at different concentrations (0, 1 fM, 10 fM, 100 fM, 1 pM, 10 pM, 100 pM, 1 nM and 10 nM) spiked in Buffer B/0.1% Nonidet P-40 and Buffer C. (B) Plot of the relationship between fluorescence ratio (F/F_0-1) at the peak value of 520 nm obtained from data (A) and the logarithm of the concentration of miR-141. (C) Fluorescence emission spectra response to the cancer cell lysates of 22Rv1 cells, DU145 cells, MDA-MB231 cells, AsPc-1 cells, BEL-7404 cells, and HeLa cells. (D) Bar representing the concentrations of miR-141 in the tested cell lysates, calculated according to fluorescence ratio (F/F_0-1) of data (C) and the linear calibration curve of data (B).

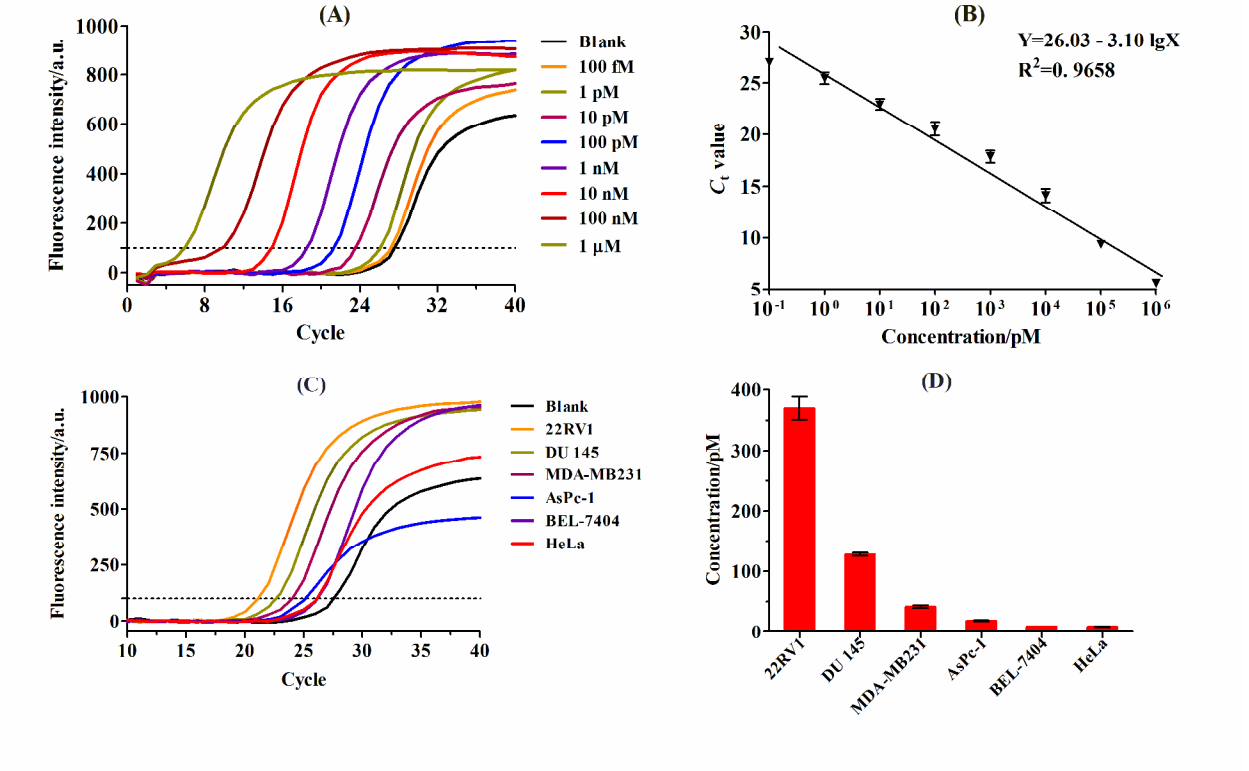

Figure S5. (A) Quantitative real-time fluorescence monitoring of the RT-PCR reactions triggered by miR-141 at different concentrations (0, 100 fM, 1 pM, 10 pM, 100 pM, 1 nM, 10 nM, 100 nM, and 1 μM) spiked in Buffer B/0.1% Nonidet P-40 and Buffer C. (B) The threshold cycle (C_t) value obtained from data (A) as a function of the concentration of miR-141. (C) Quantitative real-time fluorescence monitoring of the RT-PCR reactions triggered by cancer cell lysates of 22Rv1 cells, DU145 cells, MDA-MB231 cells, AsPc-1 cells, BEL-7404 cells, and HeLa cells. (D) Bar representing the concentrations of miR-141 in the tested cell lysates, calculated according to C_t value of data (C) and the linear calibration curve of data (B).

Table S1. Recovery results of different concentrations of miR-141 spiked in cell lysates of MDA-MB231 cells and AsPc-1 cells.

Cell line	Detected (pM)	Added (pM)	Found (pM) [a]	Recovery rate (%)
MDA-MB231	70.46	100.00	178.57±22.35	104.76
		200.00	257.50±15.04	95.21
AsPc-1	23.08	10.00	31.67±5.31	95.74
		20.00	45.14±4.43	104.78

[a] The standard deviations of measurements were calculated from three parallel experiments.